LOAD-EMBEDMENT RESPONSE OF TIMBER TO REVERSED CYCLIC LOAD

Ying H. Chui
Associate Professor

and

Chun Ni
Research Engineer

Faculty of Forestry and Environmental Management
University of New Brunswick
P.O. Box 44555
Fredericton,
New Brunswick
CANADA E3B 6C2

(Received September 1996).

ABSTRACT

One of the most important properties governing performance of timber joints containing dowel-type fasteners is the embedment response of wood under the action of a loaded fastener. Previous investigations on load-embedment behavior of wood focused almost exclusively on monotonic loading conditions. This paper describes a program of work to investigate the influence of wood density, fastener diameter, and loading characteristics on stiffness properties, ultimate strength, and strength degradation of load-embedment response of wood-based material when subjected to reversed cyclic loads. Mathematical functions were developed to describe both the envelope and hysteresis loops of the load-embedment response. A comparison of the model parameters reveals that initial stiffness and ultimate load increase with loading rate, wood density, and fastener diameter. Strength degradation occurs under both monotonic and cyclic loading for solid wood. The degree of strength degradation increases with any increase in loading rate, wood density, and fastener diameter, and presence of preloading history. No strength degradation occurs in plywood under either monotonic or reversed cyclic load.

Keywords: Embedment test, timber joints, hysteresis loops, cyclic loading, strength degradation.

INTRODUCTION

Response of mechanically fastened timber joints has been a subject of investigation by researchers for a long time. This is because joint design in timber structures quite often has a large impact on size of members in the same structure, and the design times required to detail these joints are disproportionately high in comparison with those for structural members. Previous studies focused largely on response under monotonic loading conditions. These include both theoretical (e.g., Johansen 1949; Foschi 1974; Smith 1983; Erki 1990; Koponen 1991) and experimental (e.g., Brock 1957; Mack 1966; McLain 1975; Whale et al. 1986; Komatsu 1989) studies.

Prompted by recent building failures caused by natural disasters such as hurricanes and earthquakes, the wood products industry, code writers, and building officials are increasingly aware of the need to design timber structures to withstand extreme loading conditions without catastrophic failures. As most of these loading conditions are oscillating in nature, to design for these loading conditions properly requires technical information on behavior of structural members and joints under through-zero cyclic loads. The behavior of mechanically fastened joints is of particular importance

Wood and Fiber Science, 29(2), 1997, pp. 148–160

since quite often these are the only elements in a timber structure capable of absorbing a large amount of loading energy through plastic deformation in the metal fasteners.

Recent research into the behavior of timber structures under earthquake and hurricane loading has focused primarily on behavior of timber joints. Experimental studies have been conducted on lateral resistance of nailed joints (Wilkinson 1976; Kivell et al. 1981; Soltis and Mtenga 1985; Dolan and Madsen 1991; Cruz 1993; Ni and Chui 1994) and bolted joints (Wilkinson 1976; Gutshall et al. 1994; Daneff et al. 1996). To supplement these experiments, numerical models have been developed. To date numerical joint models have been developed by Cruz (1993), Ni et al. (1993), Prion and Foschi (1994), and Ni and Chui (1996) to predict the response of a joint with a single dowel-type fastener under reversed cyclic loads. Models by Cruz (1993) and Ni et al. (1993) are simplified models based on a continuous beam bearing on a nonlinear spring foundation. The models by Prion and Foschi (1994) and Ni and Chui (1996) are more sophisticated finite element models that take into account factors such as large deformation of the fastener, localized variation of material properties, and strength degradation of the component material. As in the case of earlier models for monotonic loading, these researchers modeled a joint as a beam (fastener) bearing on a spring foundation (wood underneath fastener). The spring foundation behavior is typically characterized by the load-embedment relationship for the particular fastener size and wood type. This load-embedment behavior, therefore, is the most significant property influencing the behavior of a joint. All these models require this behavior as input.

Despite the significance of the load-embedment properties, research into this area has been very limited. For model verification purposes, Cruz (1993) performed limited tests to obtain the full load-embedment response (hysteresis) under reversed cyclic load. Ni et al. (1993); and Prion and Foschi (1994) avoided the use of cyclic loading by assuming certain simple relationships between the envelope curve, which can be obtained more easily, and the hysteresis loops. This paper describes a study to investigate how cyclic load-embedment responses are influenced by type of wood, fastener size, and loading characteristic. Part of the data was used in verifying the model by Ni and Chui (1996).

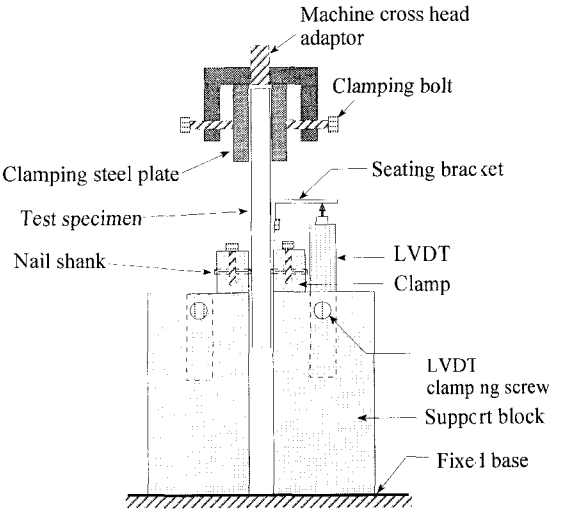

FIG. 1. Embedment test apparatus.

TEST APPARATUS

An embedment test apparatus suitable for both monotonic and reversed cyclic loading tests was developed. The test apparatus was based on the design by Cruz (1993) with some modifications. The major difference was in the gripping device. As shown in Fig. 1, the specimen is mechanically gripped by two steel plates. Clamping force was applied by tightening the steel plates with bolts. Surfaces of

TABLE 1. *Summary statistics for density and moisture content of embedment specimens.*

	Density (kg/m³)		Moisture content (%)	
Wood type	Mean	Standard deviation	Mean	Standard deviation
Spruce	474	12	11.7	0.5
Plywood	494	39	9.5	0.5
Maple	716	39	12.2	0.3

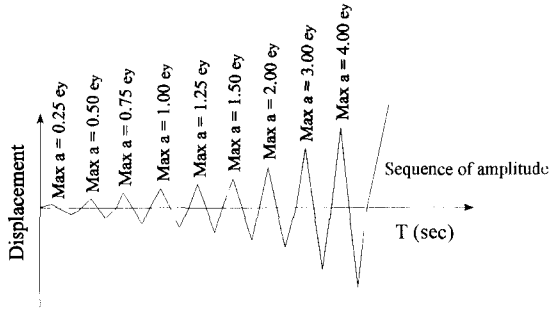

FIG. 2. Load regime 2.

the clamping plates were roughened to enhance gripping of the wood specimen. Loading was applied by a hydraulic universal test machine. In order to prevent friction, a clearance of 1 mm was maintained between the specimen and sides of the supporting steel blocks. Because of this clearance, the fastener underwent shear and bending deformations. Thus the apparatus was calibrated such that these and other extraneous deformations were subtracted from the measured response, as suggested by Whale and Smith (1989). The calibration tests were performed at a loading rate of 0.25 Hz for twenty cycles on steel specimens having the same thicknesses as the wood embedment specimens. Calibration tests were conducted for all combinations of nail size and member thickness tested in the embedment test program.

Loading of specimens was by displacement control of the loading head via a signal generator box. The generator box was programmed to provide the appropriate displacement sequence which drove the loading head. Embedment response was measured by a linear variable displacement transformer (LVDT). The applied force was measured by the test machine load cell. Signals from the test machine load cell, LVDT, and the loading head movement were recorded electronically using a computer-based data acquisition system. Data were acquired at a minimum rate of 80 samples per cycle. This ensured adequate representation of the hysteresis loops.

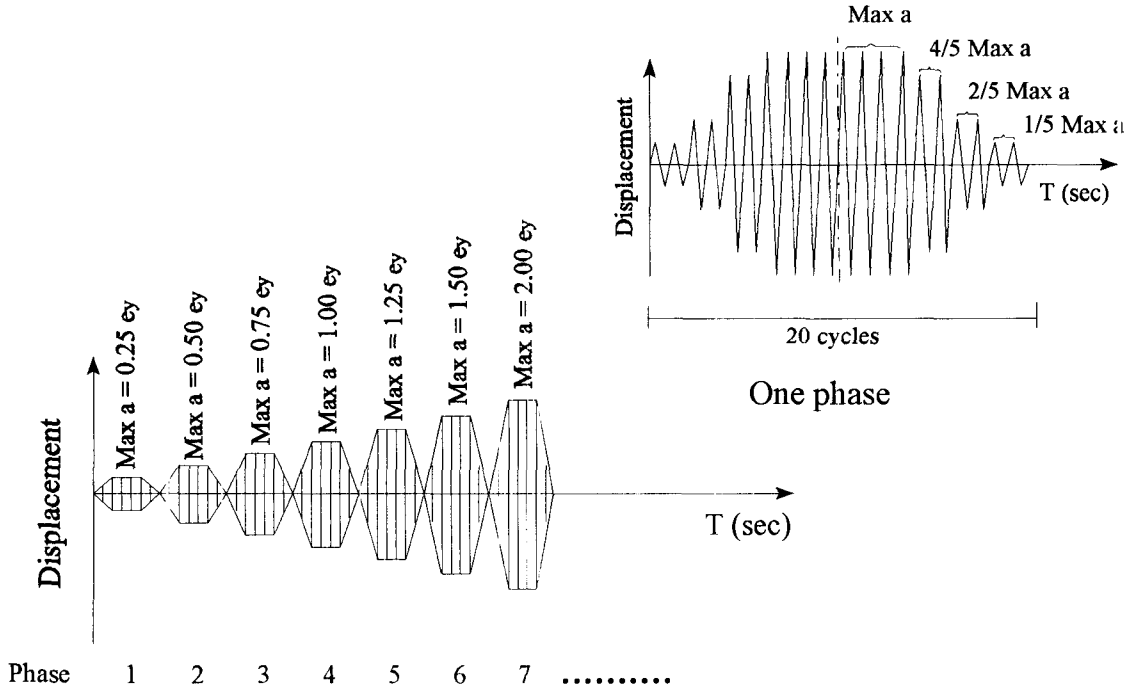

FIG. 3. Load regime 4.

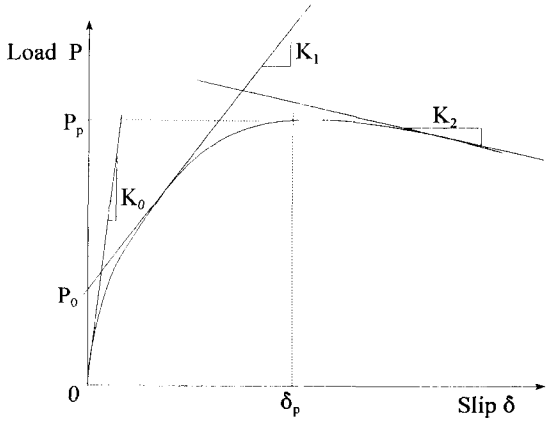

FIG. 4. Parameters of the envelope curve model.

MATERIALS AND METHODS

In order to provide a range of wood characteristics and nail sizes, three types of wood (spruce, maple, and Canadian softwood plywood) and two nail sizes (2.86 mm and 3.76 mm diameter) were tested in this study. To achieve reasonable statistical reliability in test results, ten replicates were used for each combination of wood type and nail size, and the groups of replicates for each wood type were matched based on density. For matching of samples, the sampling technique used by Smith and Whale (1989) was followed, which ensured that each group of ten replicates had similar density distribution as that of the source material. All wood materials were conditioned to 20°C and 65% relative humidity until equilibrium condition was achieved prior

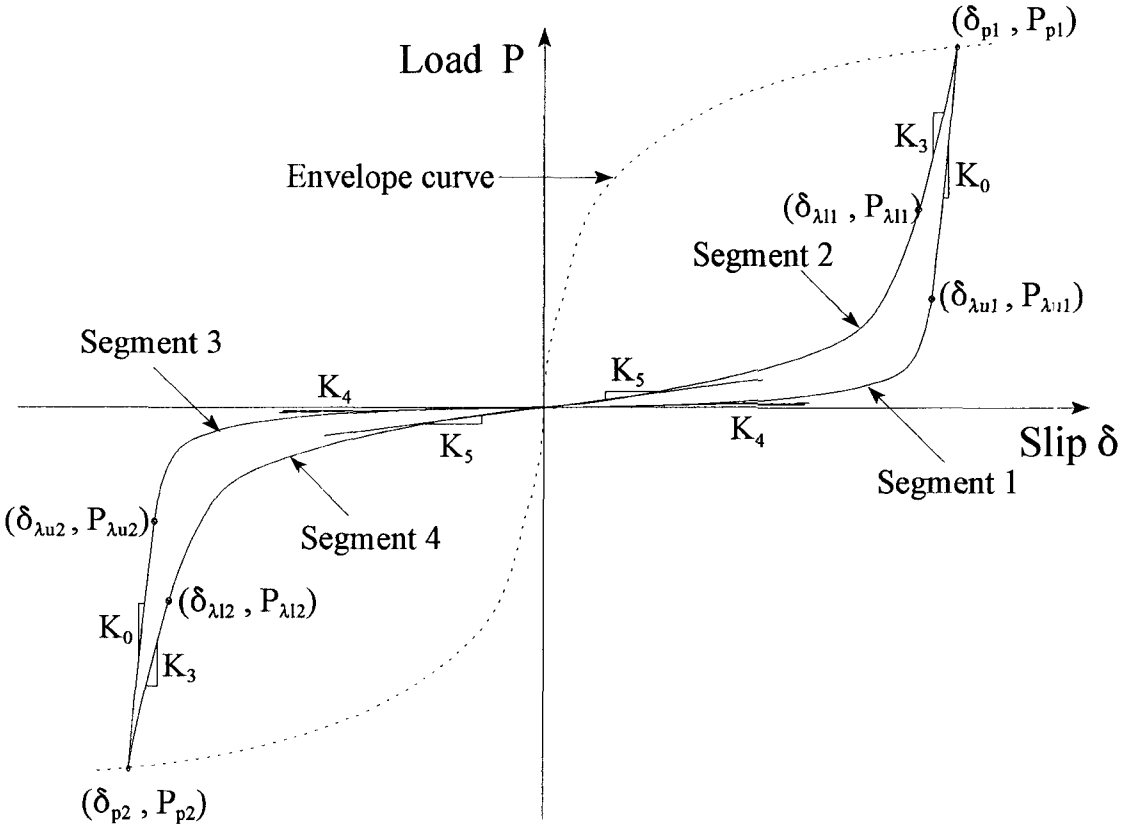

FIG. 5. Parameters of the hysteresis loop model.

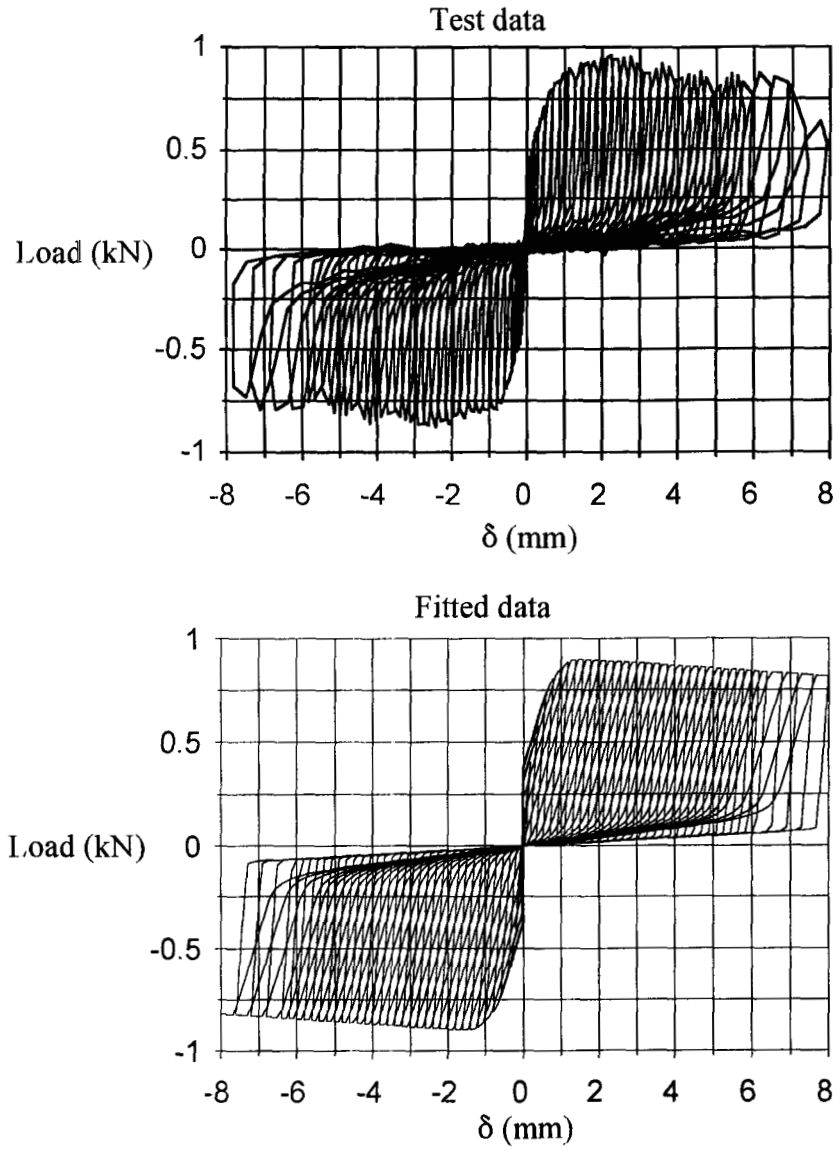

FIG. 6. A comparison of test and fitted load-embedment hysteresis data.

to testing. Table 1 summarizes the approximate means and standard deviations for density and moisture content of each type of wood specimen.

Thickness of specimens for spruce and maple was approximately twice the diameter of the nail (i.e., 5 mm for 2.86-mm nail and 7.2 mm for 3.76-mm nail). For plywood, the actual thickness (12 mm) was used. The selection of these specimen thicknesses followed the recommendations by Whale and Smith (1989). The end and edge distances of the embedment specimens were multiples of the nail diameter (d). The edge distance was 5d, and the end distances to free and grip ends were 20d and 40d, respectively. To minimize breakout of material and splitting of wood, all specimens were predrilled to 80% of nail diameter

TABLE 2. *Summary of fitted parameters for load-embedment response.*

Wood type	Fastener diameter (mm)	Loading regime	K_0 (kN/mm²)	K_1 (kN/mm²)	K_2 (kN/mm²)	K_3 (kN/mm²)	K_4 (kN/mm²)	K_5 (kN/mm²)
Spruce	2.86	1	0.398	0.0124	−0.0011	—	—	—
		2	0.504	0.0165	−0.0025	0.225	0.0018	0.0038
		3	0.534	0.0173	−0.0025	0.219	0.0017	0.0039
		4	0.453	0.0220	−0.0032	0.222	0.0015	0.0049
	3.76	1	0.582	0.0075	−0.0013	—	—	—
		2	0.790	0.0192	−0.0047	0.255	0.0006	0.0041
		3	0.822	0.0329	−0.0065	0.245	0.0009	0.0037
		4	0.621	0.0362	−0.0081	0.252	0.0008	0.0035
Plywood	2.86	1	0.285	0.0069	—	—	—	—
		2	0.352	0.0074	—	0.212	0.0005	0.0027
		3	0.360	0.0074	—	0.204	0.0005	0.0023
		4	0.292	0.0063	—	0.199	0.0005	0.0024
	3.76	1	0.455	0.0055	—	—	—	—
		2	0.506	0.0055	—	0.270	0.0005	0.0023
		3	0.531	0.0057	—	0.249	0.0006	0.0024
		4	0.461	0.0044	—	0.262	0.0007	0.0022
Maple	2.86	1	1.253	0.0023	—	—	—	—
		2	1.435	0.0092	−0.0111	0.627	0.0011	0.0056
		3	1.513	0.0312	−0.0145	0.634	0.0009	0.0067
		4	1.374	0.0057	−0.0155	0.623	0.0009	0.0055
	3.76	1	2.218	0.0036	—	—	—	—
		2	2.330	0.0588	−0.0405	0.694	0.0009	0.0069
		3	2.506	0.0918	−0.0596	0.770	0.0010	0.0060
		4	2.240	0.0733	−0.0422	0.718	0.0009	0.0058

before nailing. All specimens were loaded parallel to wood grain or face grain in the case of plywood.

To investigate the effects of loading characteristics on embedment response, four loading regimes were included. Regime 1 was a monotonic loading function with a loading rate of 2.54 mm/minute. Regime 2 was a reversed cyclic loading function with increasing peak amplitudes, as illustrated in Fig. 2. The sequence of peak amplitudes in the first few cycles was 0.25 e_y, 0.5 e_y, 0.75 e_y,, 1.0 e_y, 1.25 e_y, 1.5 e_y, 2.0 e_y, where e_y was the displacement at onset of yielding. Thereafter, amplitude was increased by one e_y until failure or a displacement of 10 mm was reached. This loading sequence followed the test procedure recommended by Reyer and Oji (1991). The rate of loading was maintained at 0.25 Hz. The value of e_y was estimated from monotonic loading tests. It was found that for all combinations of wood type and nail size, the yield point occurred at approximately 0.1 mm. This value was used in all tests. Load regime 3 had an identical loading sequence to that of regime 2, but the loading rate was doubled to 0.5 Hz. The 0.5 Hz was found to be the upper limit for pseudo-dynamic testing for the apparatus used in this study, without inducing profound inertia loading effect caused by the loading head movement. Specimens tested by load regimes 1, 2, and 3 were subjected to peak displacement that were always higher than those previously experienced by the specimens. In practice, cyclic loading from the environment such as earthquakes and hurricanes are generally pseudo-random in nature, which means that joints may be subjected to repeated peak amplitudes lower than those previously experienced. This preloading history effect may have an impact on the load-carrying capacities of timber joints. Load regime 4, as illustrated

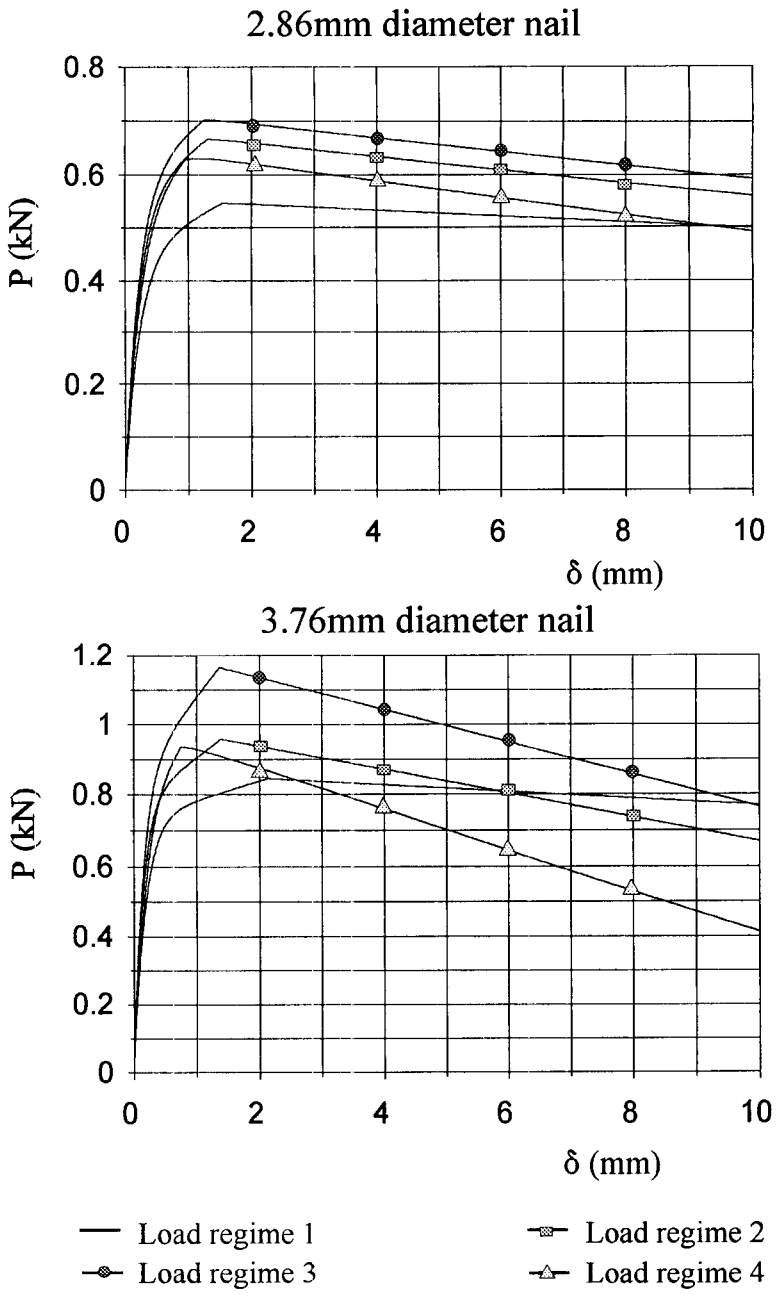

FIG. 7. Fitted envelope curves of spruce specimens.

in Fig. 3, was originally proposed by Reyer and Oji (1991) to study this preloading history effect. As can be noted from Fig. 3, load regime 4 was a phased sequential loading function, having twenty cycles of loading in each phase. Within each phase there was an initial part of 6 cycles which had increasing peak amplitudes, followed by 8 cycles of constant am-

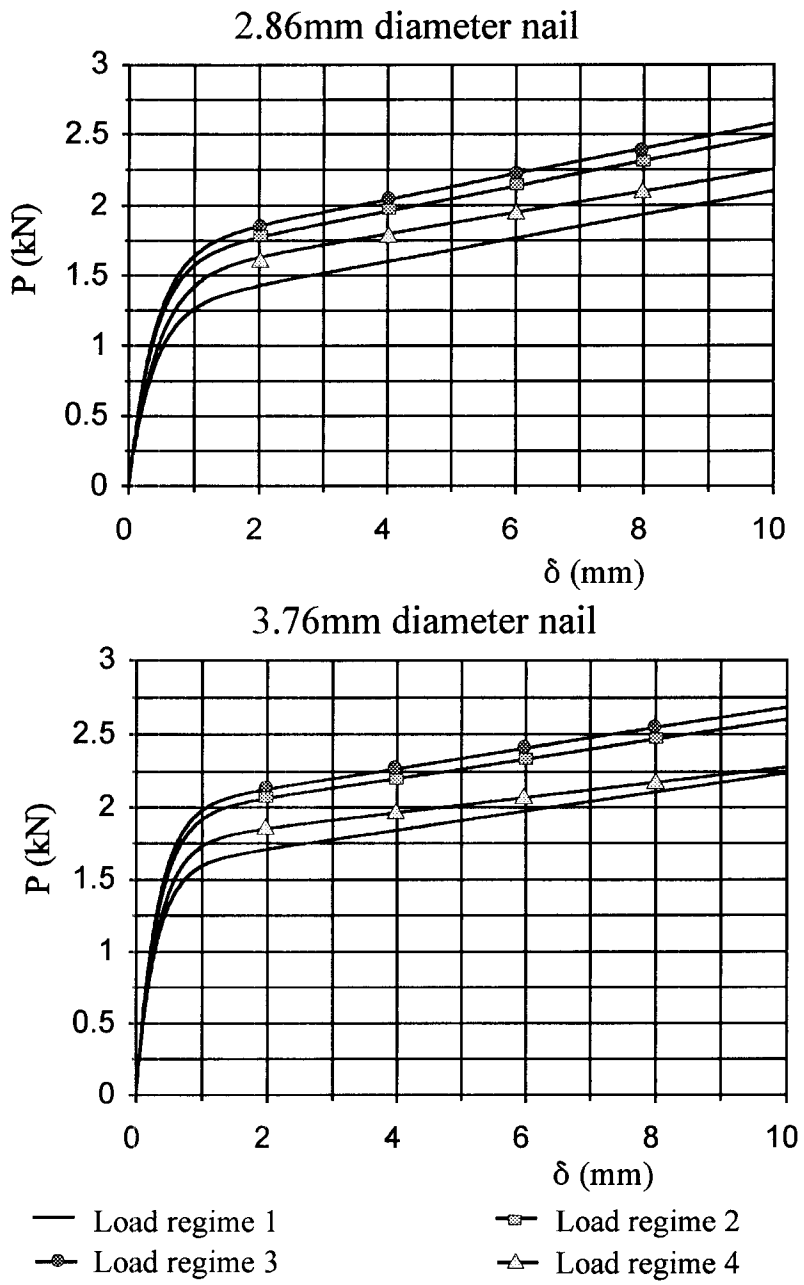

FIG. 8. Fitted envelope curves of plywood specimens.

plitudes, and then finally 6 cycles of decreasing peak amplitudes. The sequence of maximum amplitude in the loading phases followed the same pattern as in regimes 2 and 3. The loading frequency for regime 4 was 0.25 Hz.

ANALYSIS OF TEST DATA

The load-embedment data were fitted with appropriate mathematical functions. A three-parameter exponential function first proposed

by Foschi (1974) has been commonly used to describe load-slip response of timber joints under monotonic loading conditions. That function was modified by the authors to take into account the strength degradation effect. The modified form is given in Eq. (1), with the parameters defined in Fig. 4.

$$|P| = (P_0 + K_1|\delta|)\left(1 - \exp\left(-\frac{K_0|\delta|}{p_0}\right)\right) - (K_1 - K_2)(|\delta| - |\delta_p|)H(|\delta| - |\delta_p|) \quad (1)$$

where

P = load per unit length at embedment deformation δ

P_0 = intercept of the first asymptote (N/mm)

K_0 = initial stiffness (N/mm^2)

K_1 = slope of the first asymptote line (N/mm^2), Fig. 4

K_2 = slope of the second asymptote line (N/mm^2), Fig. 4

δ_p = deformation at ultimate strength

$H(|\delta| - |\delta_p|)$ = a step function, which takes the value of

$$H(|\delta| - |\delta_p|) = \begin{cases} 1 & \text{for } |\delta| - |\delta_p| \geq 0 \\ 0 & \text{for } |\delta| - |\delta_p| < 0 \end{cases} \quad (2)$$

The response under load regime 1 and the envelope curves under load regimes 2 to 4 were fitted with Eq. (1).

To completely describe the load-embedment response under reversed cyclic loads, an appropriate function is required to represent the response contained within the envelope curve, i.e., hysteresis loops. As in the nailed joint model by Dolan and Madsen (1991), four equations are used to define the four segments of each loop. Figure 5 shows a hysteresis loop with the four segments defined. Each segment is defined by four boundary conditions: the slopes at zero displacement K_4 and K_0 at maximum displacement (for unloading path), or slopes at zero displacement K_5 and K_3 at maximum displacement (for loading path), the maximum displacement reached in either direction, δ_{p1} or δ_{p2}. For those sections of the loops that are reasonably linear, they are described by straight lines.

The load-embedment relationship for segment 1 of the hysteresis loop, shown in Fig. 5, is modeled using the equation

$$P = \begin{cases} K_0(\delta - \delta_{p1}) + P_{p1} \\ \quad \text{for } \delta_{\lambda u1} \leq \delta \leq \delta_{p1} \\ \left(K_4 + \dfrac{K_0 - K_4}{1 - a_1^2}\right)\delta - \dfrac{(K_0 - K_4)\delta_{\lambda u1} a_1}{(1 - a_1^2)} \\ \quad \times \dfrac{\delta}{(1 - a_1)\delta + \delta_{\lambda u1} a_1} \\ \quad \text{for } 0 \leq \delta \leq \delta_{\lambda u1} \end{cases} \quad (3)$$

where

$$a_1 = \frac{K_0\delta_{\lambda u1} - P_{\lambda u1}}{P_{\lambda u1} - K_4\delta_{\lambda u1}} \quad (4)$$

$\delta_{\lambda u1}$ and $P_{\lambda u1}$ are the displacement and load where straight and curved segments meet.

Similar equations can be written for segments 2, 3, and 4. These are shown in Eq. (5), (7), and (9), respectively.

For segment 2

$$P = \begin{cases} K_3(\delta - \delta_{p1}) + P_{p1} \\ \quad \text{for } \delta_{\lambda l1} \leq \delta \leq \delta_{p1} \\ \left(K_5 + \dfrac{K_3 - K_5}{1 - a_2^2}\right)\delta - \dfrac{(K_3 - K_5)\delta_{\lambda l1} a_2}{(1 - a_2^2)} \\ \quad \times \dfrac{\delta}{(1 - a_2)\delta + \delta_{\lambda l1} a_2} \\ \quad \text{for } 0 \leq \delta \leq \delta_{\lambda l1} \end{cases} \quad (5)$$

where

$$a_2 = \frac{K_3\delta_{\lambda 11} - P_{\lambda 11}}{P_{\lambda 11} - K_5\delta_{\lambda 11}} \tag{6}$$

For segment 3

$$P = \begin{cases} K_0(\delta - \delta_{p2}) + P_{p2} \\ \quad \text{for } \delta_{p2} \le \delta \le \delta_{\lambda u2} \\ \left(K_4 + \dfrac{K_0 - K_4}{1 - a_3^2}\right)\delta - \dfrac{(K_0 - K_4)\delta_{\lambda u2}a_3}{(1 - a_3^2)} \\ \quad \times \dfrac{\delta}{(1 - a_3)\delta + \delta_{\lambda u2}a_3} \\ \quad \text{for } \delta_{\lambda u2} \le \delta \le 0 \end{cases} \tag{7}$$

where

$$a_3 = \frac{K_0\delta_{\lambda u2} - P_{\lambda u2}}{P_{\lambda u2} - K_4\delta_{\lambda u2}} \tag{8}$$

For segment 4

$$P = \begin{cases} K_3(\delta - \delta_{p2}) + P_{p1} \\ \quad \text{for } \delta_{\lambda l2} \le \delta \le \delta_{p2} \\ \left(K_5 + \dfrac{K_3 - K_5}{1 - a_4^2}\right)\delta - \dfrac{(K_3 - K_5)\delta_{\lambda l2}a_4}{(1 - a_4^2)} \\ \quad \times \dfrac{\delta}{(1 - a_4)\delta + \delta_{\lambda l2}a_4} \\ \quad \text{for } 0 \le \delta \le \delta_{\lambda l2} \end{cases} \tag{9}$$

where

$$a_4 = \frac{K_3\delta_{\lambda l2} - P_{\lambda l2}}{P_{\lambda l2} - K_5\delta_{\lambda l2}} \tag{10}$$

Parameters in Eqs. (3) to (10) are as defined in Fig. 5.

RESULTS AND DISCUSSION

The characterization of load-embedment response by mathematical functions is required for numerical modeling purposes. Figure 6 shows a typical comparison of test response and the fitted data. As can be noted, the model provides a good representative of the test data. Visual examinations of the embedment response showed that embedment hysteresis loops are similar to those for joints containing large diameter bolts (Gutshall et al. 1994; Daneff et al. 1996). As pointed out by Smith and Whale (1989), the embedment test can be regarded as a three-member joint with steel side plates and a thin main wood member. On the first loading to a given displacement level, the wood fibers around the fastener are compressed and crushed. Upon displacement reversal (unloading), the fastener is initially still in contact with the wood. This accounts for the high value for stiffness K_0. After a certain distance of travel, the fastener leaves the compressed wood behind and moves almost freely in the reversed direction until it contacts wood again on the opposite side. This behavior explains the low unloading stiffness (K_4) and near-zero load intercept of the loops. It is believed that the prime contributor to the stiffness is the frictional contact between side of fastener and wood. The loading segment is the reverse of this phenomenon. After a certain distance of free travel in the loading direction, the fastener bears on the wood again on the opposite side, which accounts for the sharp increase in stiffness values from K_5 to K_3.

For studying the effects of test parameters on load-embedment response, it is of interest to note the various stiffness parameters, i.e., K_0 to K_5, and the ultimate embedment load. the mean values of stiffness parameters for both envelope curve and hypteresis loop models are summarized in Table 2. Although not presented, it was noted that the coefficients of variation for these model parameters are around 10%. This relatively low variability is thought to be related to the close control of the density of the wood specimens. As was discovered by Cruz (1993), the stiffness values (K_0 and K_1) of the envelope curve increase with wood density for solid wood and with fastener diameter, except K_1 of plywood specimens, which show a reversed trend. The loading stiffness K_3 of the hysteresis loops also increases with both wood density and fastener diameter. No clear conclusions can be made with regard to effects of wood density and fastener size on K_4 and K_5. Failure to detect any sensitivity for K_4 and K_5 could be due to their small values, which make their determined

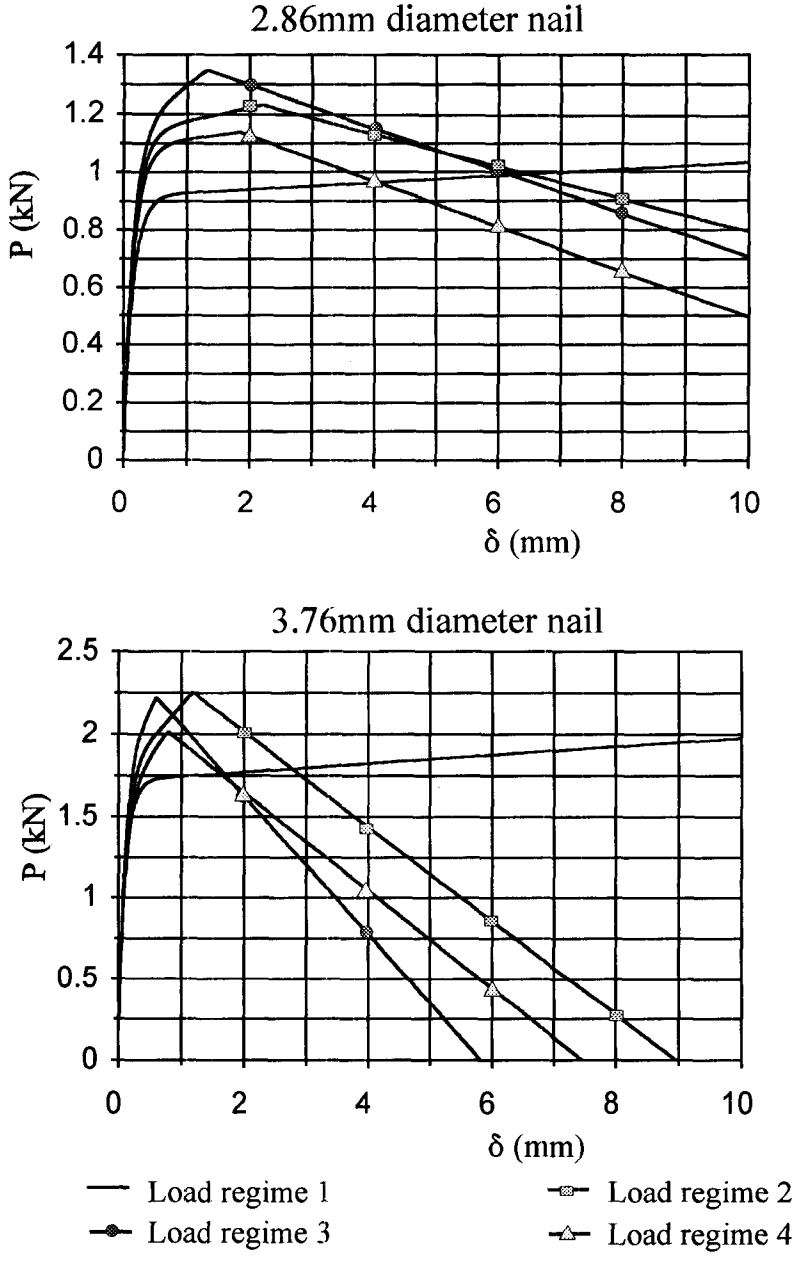

FIG. 9. Fitted envelope curves of maple specimens.

values less reliable compared with other stiffness parameters.

One of the major concerns in structural design under extreme loading conditions is the degradation of strength at high load levels. This strength degradation is characterized by the reduction in strength with increasing embedment displacement after reaching a peak force, as is illustrated in Fig. 6. In the envelope curve model, Eq. (1), this property is represented by the stiffness parameter K_2. The degrading stiffness K_2 can be easily determined

from each envelope curve by fitting a straight line through the portion of the envelope curve with $|\delta| \geq |\delta_p|$ (see Fig. 4). The effects of test parameters on ultimate load and strength degradation are better demonstrated in Figs. 7, 8, and 9 respectively for the three types of wood. Each figure shows the four fitted envelope curves under the four loading regimes. One general conclusion from the figures is that initial stiffness and ultimate load of envelope curve increase with increased loading rate. This agrees with findings from Soltis and Mtenga (1985) for nailed joints. It can be also noted from Table 2 that for each wood type and nail size, the value for K_0 is highest for load regime 3, followed by load regime 2, regime 4, and then regime 1. The value for K_0 for load regime 4 is always between that of load regime 1 and 2, indicating that the preloading history had a negative impact on initial stiffness and offsets some of the increase in stiffness due to the faster loading rate. The same conclusion can be made with regards to ultimate load prior to strength degradation.

When embedment specimens were subjected to monotonic loading, they experienced little (spruce) or no strength degradation (plywood and maple). Strength degradation occurred under reversed cyclic loading for solid wood (Figs. 7 and 9), and not for plywood (Fig. 8). The strength degradation effects are thought to be related to onset of cracking of wood material. The presence of glue planes in plywood helps to reduce cracking of wood, making it less prone to strength degradation. This may explain the excellent performance of plywood-sheathed shear wall under earthquake loading. As is evidenced by the K_2 values in Table 2 and Figs. 7 and 9, strength degradation is more pronounced in dense wood (maple) than in light wood (spruce), and in specimens loaded by a large fastener (3.76 mm) than by a small fastener (2.86 mm). The latter supports in part the general belief that, for the same overall ultimate capacity, a group of slender fasteners performs better than a group of larger diameter fasteners under reversed cyclic loading conditions. There is evidence in Table 2 to suggest also that rate of strength degradation (K_2) increases with loading rate and any preloading history.

CONCLUSIONS

The following conclusions on load-embedment properties of timber can be drawn from this study:

1. Initial stiffness of envelope curves increases with loading rate, wood density, and fastener diameter.
2. For solid wood, embedment specimens experience strength degradation in envelope curves, under reversed cyclic loads. Strength degradation is larger with denser wood and with larger fastener diameter. No strength degradation occurs in plywood embedment specimens under any of the four loading regimes.
3. Preloading history decreases stiffness and ultimate strength of load-embedment response.

ACKNOWLEDGMENTS

This study was supported by grants from the Canadian Wood Council and Natural Sciences and Engineering Research Council of Canada. Their contribution is gratefully acknowledged.

REFERENCES

BROCK, G. R. 1957. The strength of nailed joints. Forest Products Res. Bull. No. 41, Department of Science and Industrial Research, London, UK.

CRUZ, H. M. P. 1993. Nailed timber joints subjected to alternating load cycles. Ph.D. thesis, University of Brighton, Brighton, UK.

DANEFF, G., I. SMITH, AND Y. H. CHUI. 1996. Test protocol for evaluating seismic behavior of connections. Pages 37–44 *in* Proc. International Timber Engineering Conference '96, Louisiana State University, Baton Rouge, LA.

DOLAN, J. D., AND B. MADSEN. 1991. Monotonic and cyclic nail connection tests. Can. J. Civ. Eng. 19:97–104.

ERKI, M. A. 1990. Modelling the load-slip behavior of timber joints with mechanical fasteners. Ph.D. thesis, Department of Civil Engineering, University of Toronto, ON, Canada.

FOSCHI, R. O. 1974. Load-slip characteristics of nails. Wood Science 7(1):69–74.

GUTSHALL, S. T., J. D. DOLAN, AND T. E. MCLAIN. 1994. Monotonic and cyclic short-term performance of nailed and bolted timber connections. Rep. TE-1994-005, Department of Wood Science and Forest Products, Virginia Polytechnic Institute and State University, Blacksburg, VA.

JOHANSEN, K. W. 1949. Theory of timber connectors. Publications of the IABSE 9:249–262, International Association for Bridges and Structural Engineering, Zurich, Switzerland.

KIVELL, B. T., P. J. MOSS, AND A. J. CARR. 1981. Hysteretic modelling of moment resisting nailed timber joints. Bull. NZ Natl. Soc. Earthqu. Eng. 14(4):233–243.

KOMATSU, K. 1989. Behavior of nailed joints with steel side plates. Proc. Second Pacific Timber Engineering Conference, Auckland, New Zealand 2:89–94.

KOPONEN, S. 1991. Modelling the behavior of dowel type joints in wooden structures. Publ. No. 26, Laboratory of Structural Engineering and Physics, Helsinki University of Technology, Helsinki, Finland.

MACK, J. J. 1966. The strength and stiffness of nailed joints under short duration loading. Tech. Rep. No. 40, Commonwealth Scientific and Industrial Research Organization, Melbourne, Australia.

MCLAIN, T. E. 1975. Curvilinear load-slip relations in laterally loaded nailed joints. Ph.D. thesis, Colorado State University, Fort Collins, CO.

NI, C., AND Y H. CHUI. 1994. Response of nailed wood joints to dynamic loads. Proc. 1994 Pacific Timber Engineering Conference, Queensland, Australia 2:9–18.

———, AND ———. 1996. Predicting the response of timber joints under reversed cyclic load. Proc. International Timber Engineering Conference '96, Louisiana State University, Baton Rouge, LA 3:98–105.

———, I. SMITH, AND Y. H. CHUI. 1993. A simplified approach for predicting response of nailed wood joints to reversed cyclic loads. Canadian Society for Civil Engineering Annual Conference, Fredericton, NB, Canada 2:375–384.

PRION, H., AND R. O. FOSCHI. 1994. Cyclic behavior of dowel type connections. Proc. Pacific Timber Engineering Conference, Gold Coast, Australia 2:19–25.

REYER, E., AND O. A. OJI. 1991. Background document on test-methods for timber structures under seismic actions. Paper prepared for RILEM TC 109 TSA Group Meeting, London, UK.

SMITH, I. 1983. Short-term load deformation relationships for timber joints with dowel-type connections. Ph.D. thesis, Polytechnic of the South Bank, Council for National Academic Awards, London, UK.

SMITH, I., AND L. R. J. WHALE. 1989. Sampling of wood for mechanical tests on the basis of density. Mater. Struct. 22:335–338.

SOLTIS, L. A., AND P. V. A. MTENGA. 1985. Strength of nailed wood joints subjected to dynamic load. Forest Prod. J. 35(11/12):14–18.

WHALE, L. R. J., AND I. SMITH. 1989. A method for measuring the embedding characteristics of wood and wood-based materials. Mater. Struct. 22:403–410.

———, ———, AND B. O. HILSON. 1986. Behaviour of nailed and bolted joints under short-term lateral load—Conclusions from some recent research. Proc. Joint Meeting of IUFRO Wood Engineering Group and CIB-Working Commission W18, University of Karlsruhe, Germany.

WILKINSON, T. L. 1976. Vibrational loading of mechanically fastened wood joints. Res. Paper FPL 274, USDA Forest Serv. Forest Prod. Lab., Madison, WI.